

AWARD NUMBER: W81XWH-20-1-0684

TITLE: Identifying Novel Therapeutic Targets and Combination Strategies for Patients with BPDCN

PRINCIPAL INVESTIGATOR: Andrew Lane, MD

CONTRACTING ORGANIZATION: Dana-Farber Cancer Institute, Boston, MA

REPORT DATE: October 2023

TYPE OF REPORT: Annual

PREPARED FOR: U.S. Army Medical Research and Development Command
Fort Detrick, Maryland 21702-5012

DISTRIBUTION STATEMENT: Approved for Public Release; Distribution Unlimited

The views, opinions and/or findings contained in this report are those of the author(s) and should not be construed as an official Department of the Army position, policy or decision unless so designated by other documentation.

REPORT DOCUMENTATION PAGE

Form Approved
OMB No. 0704-0188

Public reporting burden for this collection of information is estimated to average 1 hour per response, including the time for reviewing instructions, searching existing data sources, gathering and maintaining the data needed, and completing and reviewing this collection of information. Send comments regarding this burden estimate or any other aspect of this collection of information, including suggestions for reducing this burden to Department of Defense, Washington Headquarters Services, Directorate for Information Operations and Reports (0704-0188), 1215 Jefferson Davis Highway, Suite 1204, Arlington, VA 22202-4302. Respondents should be aware that notwithstanding any other provision of law, no person shall be subject to any penalty for failing to comply with a collection of information if it does not display a currently valid OMB control number. **PLEASE DO NOT RETURN YOUR FORM TO THE ABOVE ADDRESS.**

1. REPORT DATE October 2023	2. REPORT TYPE Annual	3. DATES COVERED 30Sep2022 - 29Sep2023
4. TITLE AND SUBTITLE Identifying Novel Therapeutic Targets and Combination Strategies for Patients with BPDCN		5a. CONTRACT NUMBER W81XWH-20-1-0684
		5b. GRANT NUMBER
		5c. PROGRAM ELEMENT NUMBER
6. AUTHOR(S) Marina Konopleva, MD, PhD, Andrew Lane, MD, Omar Abdel-Wahab, MD		5d. PROJECT NUMBER
E-Mail: mkonople@mdanderson.org, Andrew_Lane@DFCI.HARVARD.EDU, abdelwao@mskcc.org		5e. TASK NUMBER
		5f. WORK UNIT NUMBER
7. PERFORMING ORGANIZATION NAME(S) AND ADDRESS(ES) The University of Texas MD Anderson Cancer Center, 1515 Holcombe Blvd., Houston, TX 77030 Dana-Farber Cancer Institute, 450 Brookline Avenue, Boston, MA 02215 Memorial Sloan Kettering Cancer Center, 1275 York Avenue, New York, NY 10065		8. PERFORMING ORGANIZATION REPORT NUMBER
9. SPONSORING / MONITORING AGENCY NAME(S) AND ADDRESS(ES) U.S. Army Medical Research and Development Command Fort Detrick, Maryland 21702-5012		10. SPONSOR/MONITOR'S ACRONYM(S)
		11. SPONSOR/MONITOR'S REPORT NUMBER(S)
12. DISTRIBUTION / AVAILABILITY STATEMENT Approved for Public Release; Distribution Unlimited		
13. SUPPLEMENTARY NOTES		
14. ABSTRACT Project 1: We measured characteristics of leukemia cells before and after treatment tagraxofusp (SL401) and determined that diphthamide pathway genes are silenced after tagraxofusp exposure. We also measured up-front markers of leukemia cell sensitivity to tagraxofusp and found that CD123 level correlates with baseline sensitivity but ADP-ribosylation activity of diphthamide on eEF2 by TAG does not. This suggests that diphthamide activity mediates resistance but is not a biomarker of baseline sensitivity in untreated leukemias. We also developed a BPDCN cell system for CRISPR/deadCas9 interference and performed a genome-wide CRISPRi screen for genes that affect sensitivity and resistance to tagraxofusp or venetoclax plus azacitidine. In Project 2, we have demonstrated synergistic activity combining anti-CD123 targeting agents (IMGN632 or SL401) with venetoclax and with VENetoclax and AZAcitidine, in BPDCN and AML cell lines. Mechanistic studies focusing on IMGN632/venetoclax combination have shown upregulation of apoptotic markers, profound cell cycle arrest and induction of DNA damage, which were reduced upon p53 silencing. IMGN632/venetoclax combination eradicated BPDCN in a PDX BPDCN model. We have determined the recommended phase 2 dose (RP2D) for the TAG/AZA/VEN triplet in AML/MDS trial and have recently received IRB and HRPO approval for amendment to add BPDCN cohort. We plan to initiate BPDCN enrollment in year 2 of funding period. Project 3: We determined that ZRSR2 mutations in BPDCN cells promote evasion of apoptosis by missplicing of genes in the toll-like receptor pathway, particularly the interferon response gene IRF7. This renders BPDCN cells hypoactive compared to normal pDCs in the setting of inflammation and protects them from activation-induced cell death. We have also made progress in identifying the impact of ZRSR2 mutant induced mis-splicing on immune response and generation of potentially immunogenic proteins that could serve as exciting potential immunotherapy targets.		

15. SUBJECT TERMS Blastic Plasmacytoid Dendritic Cell Neoplasm (PBDCN), Acute Myeloid Leukemia (AML), CD123, tagraxofusp, IMG632, venetoclax, azacytidine, combination therapy,					
16. SECURITY CLASSIFICATION OF:			17. LIMITATION OF ABSTRACT	18. NUMBER OF PAGES	19a. NAME OF RESPONSIBLE PERSON
a. REPORT	b. ABSTRACT	c. THIS PAGE	UU	33	USAMRDC
U	U	U			19b. TELEPHONE NUMBER <i>(include area code)</i>

Standard Form 298 (Rev. 8-98)
Prescribed by ANSI Std. Z39.18

TABLE OF CONTENTS

	<u>Page</u>
1. Introduction	5
2. Keywords	5
3. Accomplishments	5
4. Impact	30
5. Changes/Problems	31
6. Products	31
7. Participants & Other Collaborating Organizations	33
8. Special Reporting Requirements	41
9. Appendices	41

1. INTRODUCTION:

BPDCN is a highly aggressive hematologic malignancy characterized by poor clinical outcomes and no approved or standard therapies. It can evolve out of an underlying myelodysplastic syndrome or present de novo. The median age is ~65 years with overall survival of 8-14 months using conventional chemotherapy. Thus, there is an urgent unmet need for rational targeted agents and non-cytotoxic therapies. CD123 (the IL3 receptor) is highly expressed in ~100% of BPDCN cases, generally at higher levels than normal cells or forms of acute myeloid leukemia (AML). This observation led to a multi-center Phase I/II trial of SL-401 (Tagraxofusp) in BPDCN, which our sites led and recent FDA approval of tagraxofusp (Elzonris™, Stemline Therapeutics, Inc.), a CD123-directed cytotoxin. Among 45 patients, we observed a 72% combined rate of complete response (CR)/clinical complete response in frontline-treated patients and 38% in relapsed patients; 45% of frontline patients were bridged to stem cell transplant.⁴ However, many patients experience relapse after initial response to tagraxofusp, and ~30% of patients do not respond to tagraxofusp monotherapy up-front. Preliminary studies indicate that BPDCN is dependent on BCL-2. In BPDCN cell lines, patient samples, patient-derived xenograft (PDX) models, and a two-patient pilot study, we observed a high sensitivity to the BCL-2 inhibitor venetoclax. Since then, there have been subsequent reports of clinical activity against BPDCN with venetoclax as a single agent, or in combination with hypomethylating agents. Although we have observed activity of anti-CD123 and anti-BCL-2 targeted agents as *monotherapies*, relapses still occur in most cases. **This project aims to** investigate mechanisms of response and resistance to the most advanced targeted therapies in BPDCN, assess potential for combination treatment in a clinical trial, and explore novel mechanism-based therapies targeting recurrently mutated genes in BPDCN involved in RNA splicing. **We expect our aims to provide clinical data for the next front-line treatment strategy for BPDCN patients and the preclinical basis to intelligently select the next targeted therapy approach for clinical testing in BPDCN.**

2. KEYWORDS:

Blastic Plasmacytoid Dendritic Cell Neoplasm (BPDCN), Acute Myeloid Leukemia (AML), CD123, tagraxofusp, IMGN632, venetoclax, azacytidine, combination therapy

3. ACCOMPLISHMENTS:

What were the major goals of the project?

Specific Aim 1

Major Task 1: Test the hypothesis that in vivo resistance to tagraxofusp in BPDCN cells is mediated by epigenetic silencing of diphthamide synthesis genes.

Major Task 2: Test the hypothesis that azacitidine cooperates with tagraxofusp in primary BPDCN cells in vivo via its effects on DNA methylation and expression of diphthamide synthesis genes.

Specific Aim 2

Major Task 1 Test the hypothesis that targeting of CD123 with tagraxofusp or IMGN-623 primes BPDCN cells for apoptosis when combined with BCL2 inhibitor venetoclax and AZA.

Major Task 2 Determine the efficacy of combining anti-CD123 therapy with AZA/venetoclax in vivo

Major Task 3 Conduct a Phase 1b/2 clinical trial combining azacitidine, tagraxofusp, and venetoclax in patients with relapsed/refractory BPDCN and frontline patients unfit for induction chemotherapy

Specific Aim 3

Major Task 1: Determine the effects of perturbing splicing in BPDCN models with or without mutations in *ZRSR2* or *SRSF2*.

Major Task 2: Determine aberrant splicing events generated by mutant *ZRSR2* and *SRSF2* in BPDCN which promote transformation through a positive enrichment CRISPR screen.

What was accomplished under these goals?

Specific Aim 1, Major Tasks 1 and 2:

We have made continued progress on Aim 1 goals during this reporting period and have met all goals. The major focus over the last year has been following up on hits from a genome-wide CRISPR interference screen to determine new ways to sensitize BPDCN cells to existing therapies and overcome resistance to those therapies.

We have been focusing on a gene from our CRISPR screen that was shared as the top hit between tagraxofusp and venetoclax/azacitidine treated BPDCN cells. That hit is an RNA binding protein called KHSRP that when knocked down, increases the susceptibility of BPDCN cells to both therapies/combinations.

First, we performed an integrated analysis of RNA sequencing from BPDCN PDXs treated in vivo with tagraxofusp or venetoclax/azacitidine with the CRISPR interference screen results. From a pathway standpoint, there was clear overlap, suggesting that the residual disease cells in vivo indeed have shared biology with the CRISPR enriched or depleted genes from in vitro drug sensitivity/resistance screening. For example, the residual population in vivo by transcriptomics was highly enriched for oxidative phosphorylation (OXPHOS) and epithelial-mesenchymal transition (EMT) features. In the CRISPRi screen, 66 enriched hits (promoted resistance) were in mitochondrial respiration pathways. Since this finding was consistent with what has been reported in AML and validates the assay, we have focused on the depleted hits. In other words, we chose

genes that when knocked down cooperate with tagraxofusp or VEN/AZA to kill BPDCN cells. There were 15 depleted hits in the CRISPRi screen and KHSRP was the top gene.

In recent months, we have focused on KHSRP biology, specifically in BPDCN cells and in settings in the setting of drug treatment. First, we have begun to investigate whether KHSRP localization to stress granules is important or involved in the drug sensitivity response. Stress granules (SGs) are dense cytoplasmic hubs of protein and RNA activity that are increased in size during cellular stress. We developed an immunofluorescence assay to test for KHSRP localization and for stress granule appearance. We found that VEN/AZA treatment induced stress granule formation in CAL1 BPDCN cells, as measured by cytoplasmic translocation of G3BP1, a canonical SG protein (**Figure 1**). In contrast, at least at the time points measured (early after treatment), KHSRP did not appear to move from the nucleus to cytoplasm or co-localize with G3BP1 or SGs in treated cells.

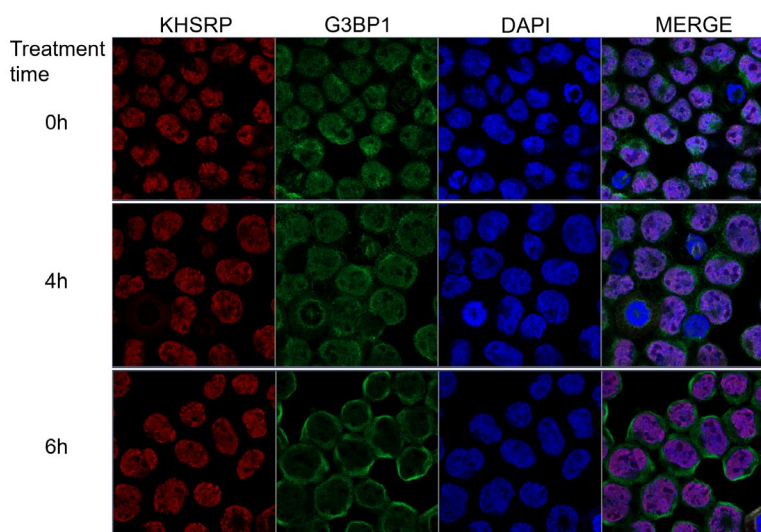


Figure 1. Immunofluorescence in CAL1 BPDCN cells at the indicated times after lethal doses of VEN/AZA in combination (but at early time points prior to cell death). G3BP1 is a canonical stress granule protein that localizes to the cytoplasm after chemotherapy treatment.

The second major effort has been to analyze eCLIP-seq data for RNAs that bind to KHSRP. KHSRP is known as an RNA binding protein although it is possible that its effects to mediate drug resistance are related or not related to RNA binding. We performed an IP with anti-KHSRP antibodies that have been validated in the setting of KHSRP knockout vs control IgG, each after treatment with VEN/AZA or DMSO controls. Each was performed in duplicate. The data were high quality with >4900 specific peaks detected in each condition (**Figure 2, top**). We have begun to analyze these peaks for their overlap with RNA-sequencing of KHSRP wild-type vs knock in cells and in the setting of various drug treatments, and for overlap with our genomewide CRISPRi screen hits. An example of an enriched RNA is shown below, where there is clear and antibody-specific binding of KHSRP to this RNA and possibly decreased binding in the setting of VEN/AZA treatment (**Figure 2, bottom**).

D. Quality control metrics:

Notes: A peak is defined as a cluster with \log_2 fold enrichment ≥ 3 and p-value ≤ 0.001

Sample ID Name	Initial reads	% pass adapter trim	% repetitive elements	% aligned uniquely to genome	% PCR duplicates	Final reads	Number of clusters	Number of input normalized peaks
DMSO_IP_Rep1	44,946,579	97.76%	28.09%	71.95%	13.86%	19,582,891	527,082	11,856
DMSO_IP_Rep2	47,928,659	97.98%	36.35%	68.21%	11.58%	18,026,663	514,082	4,900
DMSO_Input_Rep1	45,300,278	98.78%	77.31%	49.69%	6.53%	4,716,354	NA	NA
DMSO_Input_Rep2	51,841,320	99.55%	77.03%	56.29%	4.82%	6,352,567	NA	NA
VenAza_IP_Rep1	45,142,928	97.54%	35.66%	69.24%	17.04%	16,273,513	473,332	5,135
VenAza_IP_Rep2	49,357,514	98.73%	37.18%	67.55%	9.81%	18,650,938	515,591	5,129
VenAza_Input_Rep1	48,321,727	99.45%	80.16%	52.55%	4.55%	4,782,748	NA	NA
VenAza_Input_Rep2	55,615,302	99.71%	79.82%	55.21%	3.43%	5,965,966	NA	NA

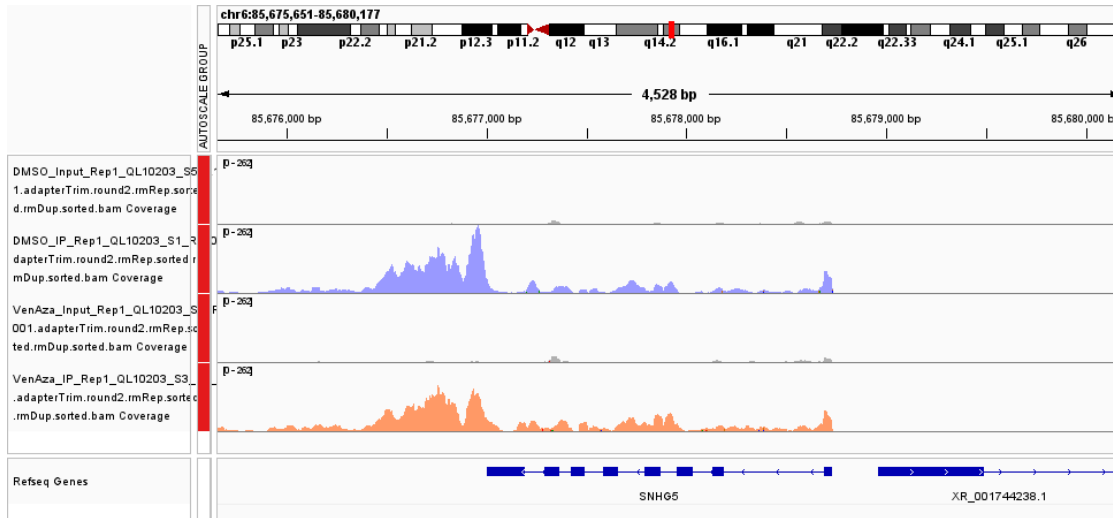


Figure 2. (Top) Quality metrics and peak calls for anti-KHSRP eCLIP-seq. (Bottom) Example gene tracks from eCLIP-seq for an RNA that binds to KHSRP, showing specificity over IgG controls (input) and in the setting of drug treatment (VEN/AZA or DMSO vehicle control).

We have also validated that the drug sensitization effect was indeed due to KHSRP loss with individual knockdown using multiple sgRNAs. We confirmed necessity and sufficiency with knockdown and add back experiments. Knockdown of KHSRP led to sensitization of BPDCN cells (CAL1) to treatment with either tagraxofusp or venetoclax plus azacitidine (**Figure 3a-b**). Interestingly and importantly, knockdown of KHSRP alone did not affect the growth of untreated CAL1 cells (**Figure 3c**), suggesting this was not a general toxic effect and rather a true drug sensitization effect.

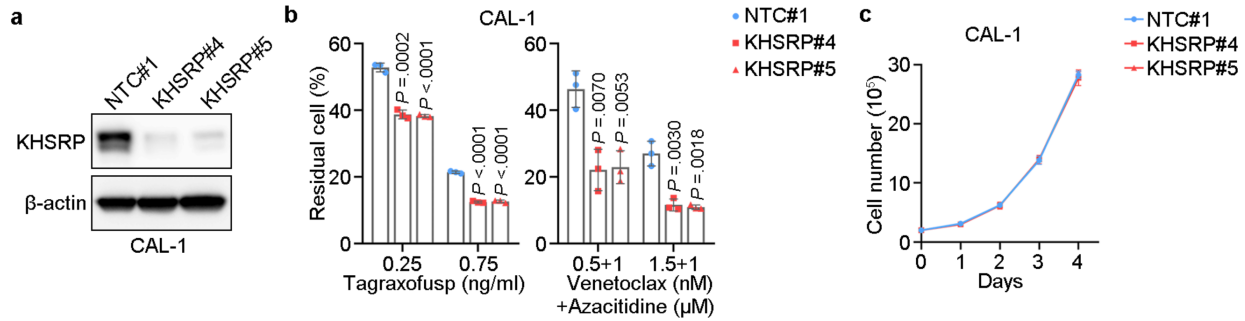


Figure 3. KHSRP knockdown sensitizes BPDCN cells to tagraxofusp and venetoclax/azacitidine. a, CRISPR interference knockdown of KHSRP with independent sgRNAs in CAL1 cells. b, Sensitization of BPDCN cells to tagraxofusp or venetoclax and azacitidine by KHSRP knockdown. c, Growth of BPDCN cells at baseline is not affected by KHSRP knockdown.

We have also performed deeper analysis of the combined eCLIPseq and transcriptomics experiments. The goal was to test which RNAs are directly bound by KHSRP, both at baseline and in the setting of VEN/AZA treatment, compared to input controls. We have also been analyzing RNA-sequencing in the same conditions, to nominate gene targets that may be affected by the RNA binding properties of KHSRP that could mediate downstream drug sensitivity (**Figure 4**). One new top target we have been investigating during this reporting period is the solute carrier SLC23A1, which is activated in the setting of KHSRP knockdown (**Figure 4b**). Interestingly, SLC23A1 is a transporter for ascorbic acid, or Vitamin C, which has been linked to leukemia cell growth, differentiation, viability, and particularly, to sensitization to targeted therapy in other contexts. We also found that SLC23A1 is suppressed in measurable residual disease (MRD) BPDCN cells after targeted therapy treatment in vivo (in patient-derived xenografts; **Figure 4c**).

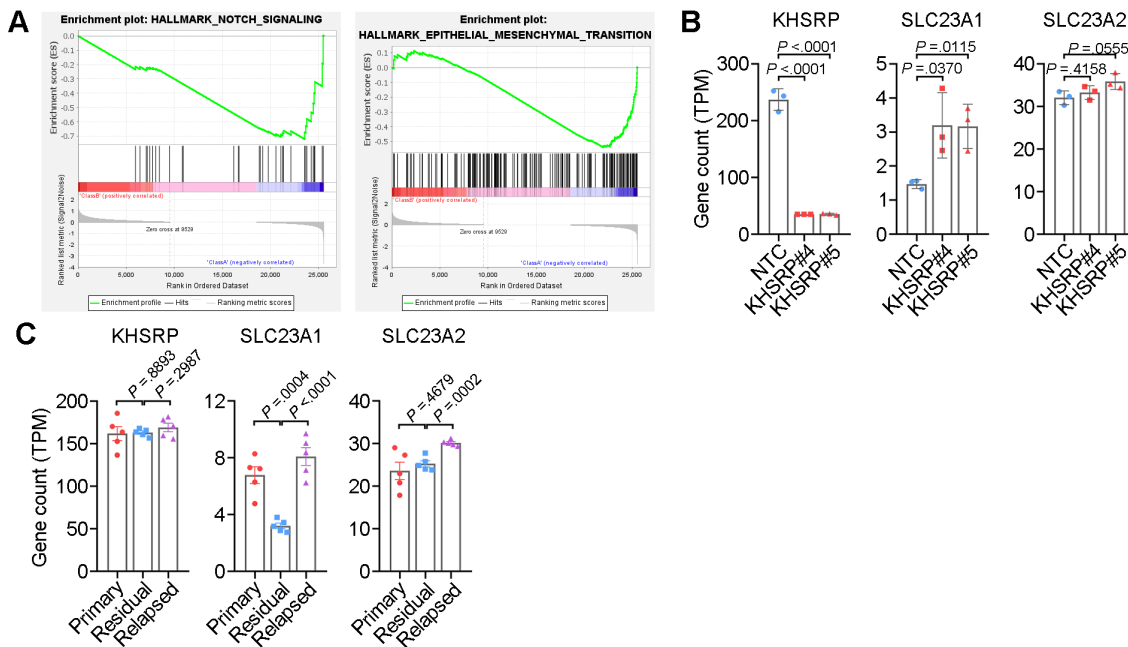


Figure 4. Transcriptional consequences of KHSRP knockdown in BPDCN cells. a, GSEA enrichment in BPDCN cells following KHSRP knockdown reveals transcriptional program changes

consisted with activation of signaling pathways such as via Notch and features of epithelial-mesenchymal transition. b, SLC23A1 has increased expression in BPDCN cells following KHSRP knockdown, but there is no change in the closely related SLC23A2. c, Analysis of patient PDXs from BPDCN treated in vivo with VEN/AZA shows that SLC23A1 is specifically repressed in measurable residual disease (MRD) cells compared to baseline or at progression after treatment.

Finally, eCLIP-seq suggested that KHSRP binds directly to the SLC23A1 mRNA, particularly at the 5'UTR and 3'UTR (**Figure 5**). Together, this suggests a testable model wherein KHSRP protects BPDCN cells from therapy with tagraxofusp or venetoclax and azacitidine, possibly via suppression of SLC23A1 and decreased transport of ascorbic acid. Sensitization to these therapies could therefore be achieved by knockdown of KHSRP and/or treatment with ascorbic acid/Vitamin C. We will evaluate these possibilities in planned experiments, plus perform more detailed validation of the role of the therapy-induced residual disease – KHSRP – SLC23A1 – ascorbic acid axis.

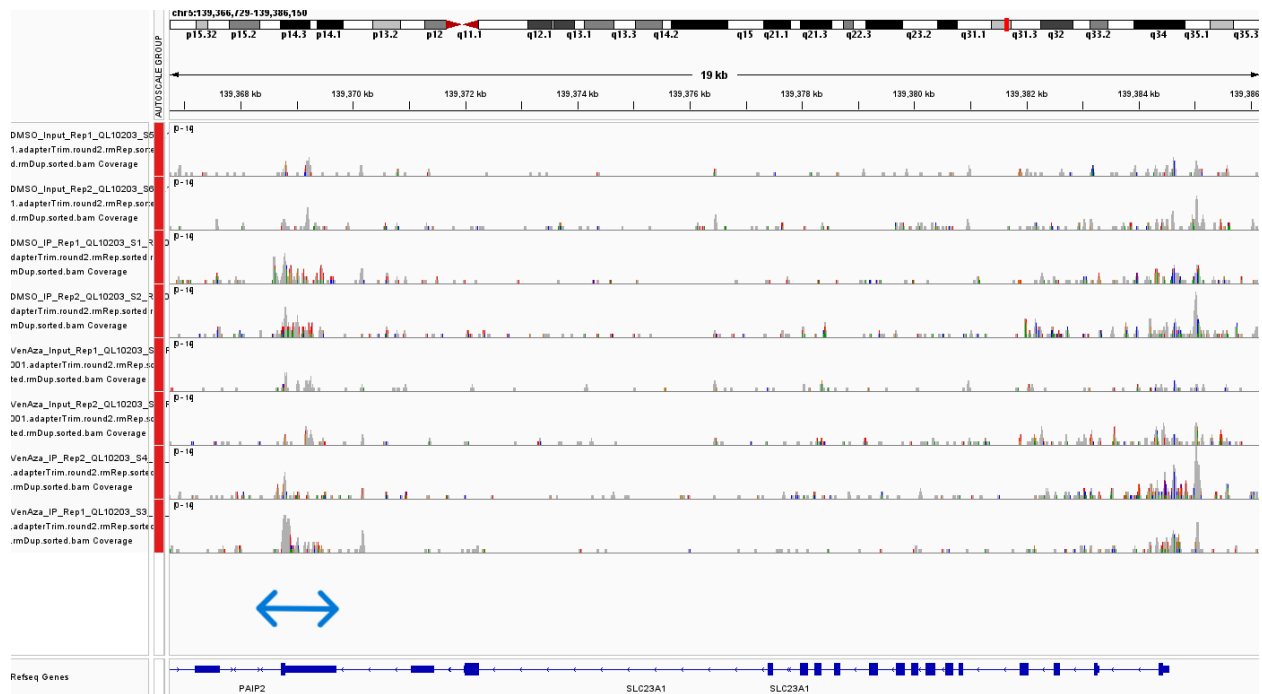


Figure 5. eCLIP-seq reveals binding of KHSRP to SLC23A1 mRNA in DMSO or VEN/AZA-treated BPDCN cells, relative to input controls. The blue arrow represents an area of binding in the SLC23A1 3'UTR in both immunoprecipitation conditions over input controls. Each condition was performed with independent biological duplicates, which are represented in paired rows.

We continued to explore additional integrated analysis of results from two datasets: 1) an experiment quantifying gene expression changes at minimal residual disease timepoints and relapse in BPDCN patient derived xenografts after venetoclax and azacitidine combination or tagraxofusp. And 2) a genome wide CRISPR interference screen in BPDCN cells to test genes that influence early timepoints (mimicking MRD assessments) of sensitivity and resistance to VEN/AZA or tagraxofusp. **Figure 6** shows top hits from the two CRISPR interference screens. Panel G (left) shows VEN/AZA hits: in blue are genes that when knocked down caused resistance to VEN/AZA.

These include expected hits in the mitochondrial apoptosis pathways like BAX and NOXA, as well as TP53, a known resistance gene for venetoclax. Expected sensitizing knockdown was (in red) was achieved with loss of MCL1, BCL2L1, and MDM2. On the right panel are expected resistance genes (blue) to tagraxofusp including the IL3 receptor alpha and beta chains and the diphthamide genes DPH1 and DPH4. Most striking is the top overlapping sensitizing gene, KHSRP, as detailed above.

Next, we looked for overlapping gene sets (panel H) by Gene Ontology terms that were shared between VEN/AZA and TAG treatment arms. Among the top shared gene sets are protein translation control genes. KHSRP is known to affect RNA translation. We also found several oxidative phosphorylation gene sets and genes in our RNA seq plus CRISPR hits, which is not unexpected from studies of venetoclax. Interestingly, when we separate short term treated BPDCN cells after TAG or VEN/AZA into Annexin V positive (undergoing apoptosis) and negative (remaining healthy) fractions, KHSRP was maintained or even increased in the fully resistant populations (Annexin V negative) but was lower in the apoptotic cells. OX PHOS proteins were upregulated as has been reported after venetoclax treatment, but this was in the cells already undergoing apoptosis (panel I). This led us to conclude that KHSRP may be truly associated with resistance to TAG and VEN/AZA, whereas OX PHOS gene upregulation may be more associated with cells committed to death, at least at these MRD time points. Therefore, we have focused on understanding the mechanism by which KHSRP is protecting BPDCN cells from TAG and VEN/AZA.

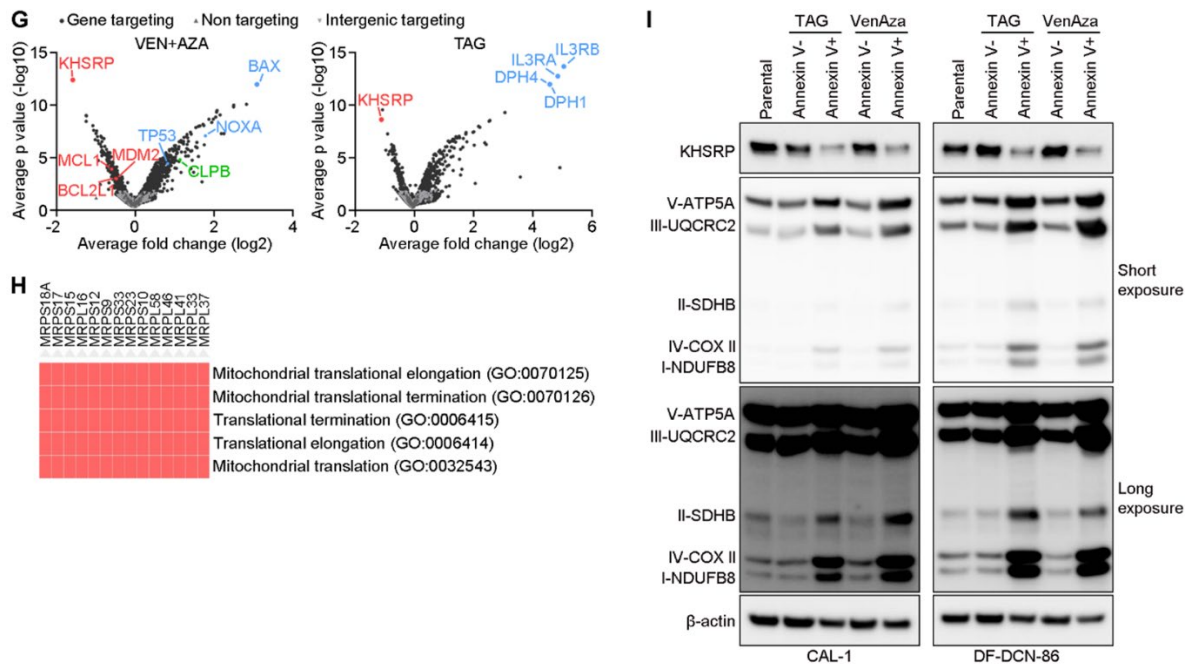


Figure 6. G) Summary of the CRISPR screen hits for sensitizers (red) and resistance genes (blue) to VEN/AZA or TAG treatment in BPDCN cells. H) Overlap of the Gene Ontology terms that are associated with resistance to both treatments. I) Western blotting for KHSRP and the indicated oxidative phosphorylation enzymes in two BPDCN cell lines after treatment with TAG or VEN/AZA, sorted by Annexin V negative and positive fractions.

We performed further analyses of BPDCN cells after KHSRP knockdown to identify possible downstream consequences that might be associated with resistance to therapy. Several of the notable gene sets and individual genes are shown in **Figure 7**. Several lines of evidence have directed us to the solute carriers SLC23A1 and SLC23A2. These genes encode proteins that regulate the cell membrane transport of Vitamin C into the cytoplasm. Of interest yet without additional data at this time, is that Vitamin C has been linked to leukemia cell survival and to mutations in TET2, which are present in >70% of BPDCNs and frequently biallelic whereas in other leukemias TET2 mutations are rarely biallelic. SLC23A1 (but interestingly not SLC23A2) is consistently associated with KHSRP levels and response to therapy in BPDCN cells. In Panel E and D of Figure 2, we see that SLC23A1 is suppressed in therapy resistant BPDCN PDXs in vivo and is activated by KHSRP knockdown. As above, we also showed eCLIP-seq data that KHSRP may bind to the SLC23A1 mRNA directly. We are currently attempting to validate this binding by direct IP and RT-PCR, as well as test if binding may be modulated in the setting of chemotherapy treatment.

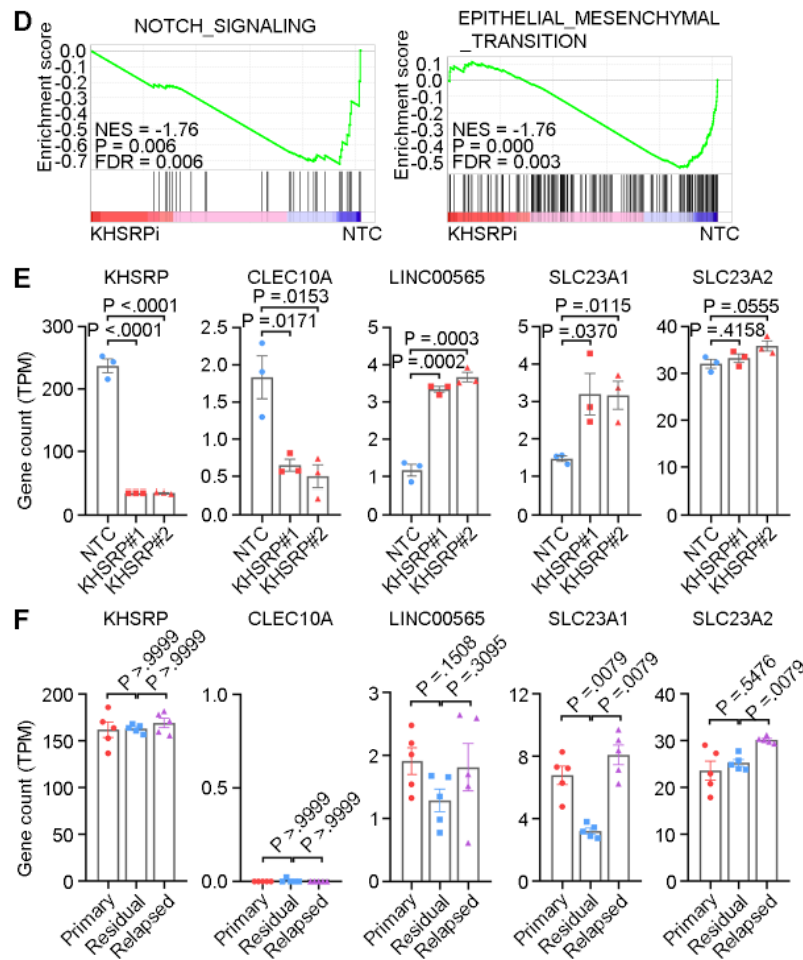


Figure 7. D) RNA-seq gene set enrichment analysis comparing KHSRP knockdown to control cells. E) RNA-seq of the indicated genes after KHSRP knockdown. F) RNA-seq of the indicated genes in primary, MRD (residual), and relapsed BPDCN PDXs in vivo after treatment with VEN/AZA.

We have also begun to perform mechanism-based studies to test if SLC23A1 and/or SLC23A2 are important for the effect of KHSRP in BPDCN cells undergoing therapy. In **Figure 8** we see the combined effect of KHSRP knockdown (by CRISPR interference) with SLC23A1 or SLC23A2 knockdown (by shRNA). Panel G shows confirmation that the shRNAs knock down the genes of interest. Panel H shows that loss of KHSRP sensitizes to VEN/AZA and TAG, as expected from the CRISPR interference screen. It also shows that loss of SLC23A1 or SLC23A2 completely blocks the ability of VEN/AZA or TAG to kill BPDCN cells in the presence of loss of KHSRP. This raises several new questions that will be addressed in the future directions section below. These include whether Vitamin C is indeed the critical solute carried by SLC23A1/2 to modulate drug sensitivity, or whether another candidate may mediate the effect. This is particularly intriguing because standard cell culture media (as used here) is considered to lack Vitamin C.

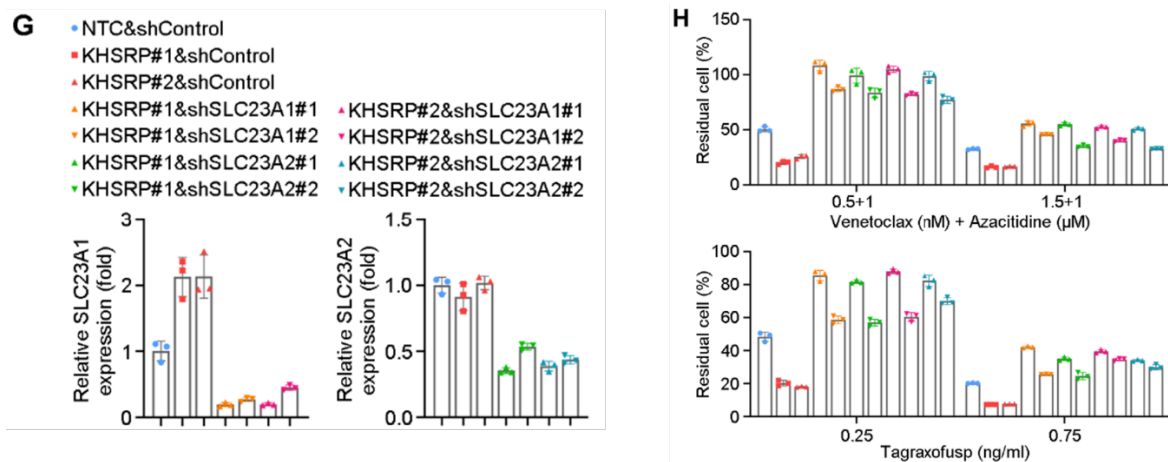


Figure 8. G) Quantitative RT-PCR for the indicated genes in the setting of CRISPRi for KHSRP vs control, and/or knockdown of SLC23A1 or SLC23A2, as indicated. H) Cell number after treatment with two different concentrations of VEN/AZA or TAG, as indicated, in cells with the same CRISPR interference/shRNA combinations as in panel G.

Specific Aim 2, Major Task 1: Test the hypothesis that targeting of CD123 with tagraxofusp or IMGN-623 primes BPDCN cells for apoptosis when combined with BCL2 inhibitor venetoclax and AZA.

We have made continued progress on Aim 2 goals during this reporting period and focused over the last year on establishing mechanism of synergy between IMGN632 and venetoclax. We have previously shown that IMGN632 alone, as well as in combination with VEN/AZA, induced profound double-stranded DNA damage, which triggered activation of DNA-damage response sensors, p53 and Chk1, preventing cells from entering S-phase. While single agent VEN treatment produced similar level of p- γ H2AX, the drug neither triggered phosphorylation of p53 nor substantial phosphorylation of Chk1. Upon combined IMGN632+VEN treatment, p53 phosphorylation was sustained, but phosphorylated Chk1 decreased with time, suggesting that VEN may impair DNA damage response initially triggered by IMGN632, which in the presence of elevated DNA damage, can lead to enhanced leukemia cell killing. To support this hypothesis, in current reporting period, we examined whether/how sequence of IMGN632 and VEN exposure may affect the efficacy of tested combination. MV4-11, MOLM13 and MOLM14 AML cells were pretreated for 24h with either IMGN632 or VEN alone, followed by 24-hour exposure to IMGN632 or VEN, respectively. For

comparison, IMGN632 and VEN were also given simultaneously for 48h. Cell viability was assayed by CellTiter-Glo assay and synergistic interactions were calculated using SynergyFinder software. BLISS index values for each dose combination >0 represented synergy, whereas BLISS index values <0 represented antagonism. As shown in the heat maps (Figure 9), pre-treatment of AML cells with IMGN632 prior to VEN administration had significant synergistic effect at multiple dosage levels and ratios, which was comparable to the effect observed upon simultaneous IMGN632/VEN exposure. In contrast, pre-treatment with VEN for 24h followed by IMGN632 profoundly decreased the efficacy and strong synergy of IMGN632/VEN combination, indicating the importance of sequence for using these two drugs to maximize the antileukemic effect.

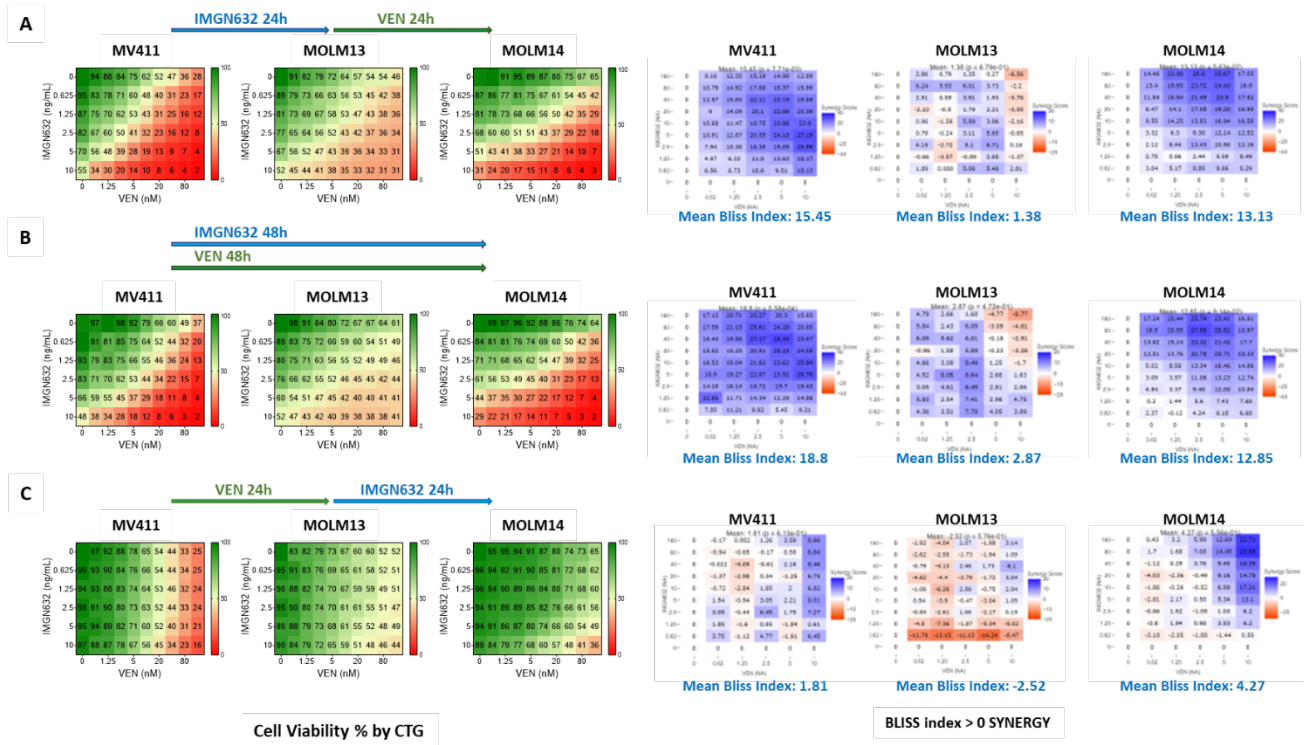


Figure 9. The effect of sequence of IMGN632 and VEN treatment in AML cells. (Left) AML cells were (A) pretreated with IMGN632 for 24 h followed by 24h VEN, (B) simultaneously treated with IMGN632 and VEN for 48h or (C) pretreated with VEN for 24h followed by 24h IMGN632. Cell viability was measured using CellTiterGlo assay. (Right) Heat maps of Bliss synergy index. Blue coloration indicates synergistic drug combinations, white areas indicate additive effect, and red – antagonistic effect.

In parallel, we also tested the role of other components of DDR upon IMGN632 and VEN treatment. Surprisingly, IMGN632 exposure led to rapid dephosphorylation of Chk2 kinase, indicating on inactivation of ATM/Chk2 DDR pathway (Figure 10).

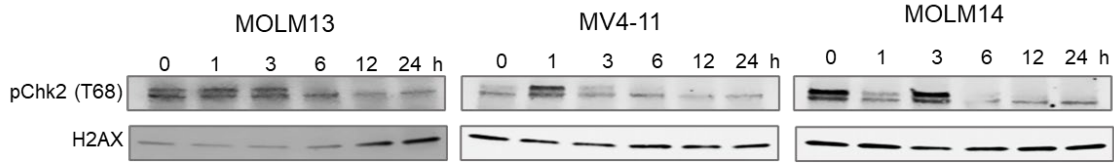


Figure 10. Western blot analysis of pChk2 kinase, a component of ATM/ChK2 DNA damage response AML cells treated with 2.5 ng/mL IMGN632 for up to 24 h.

As shown in Figure 11, IMGN632 significantly increased nuclear expression of RAD51 recombinase, which is a critical effector of homologous recombination, an essential DNA repair mechanism for double-strand breaks during S and G2 phase of the cell cycle. RAD51 also plays non-repair functions at stalled replication forks, in which RAD51 stimulates fork reversal and stabilizes stalled forks by protecting against the nucleolytic degradation of nascent DNA (Wassing IE, Nature Commun 2021). Importantly VEN co-treatment decreased the level of Rad51. Similarly, combined IMGN632 and VEN led to downregulation of Wee1 kinase, which plays a crucial role in the G2-M cell cycle checkpoint arrest for DNA repair before mitotic entry. Together, these results suggest that VEN may potentiate the cytotoxic effect of IMGN632 by suppressing the DNA damage repair in AML cells.

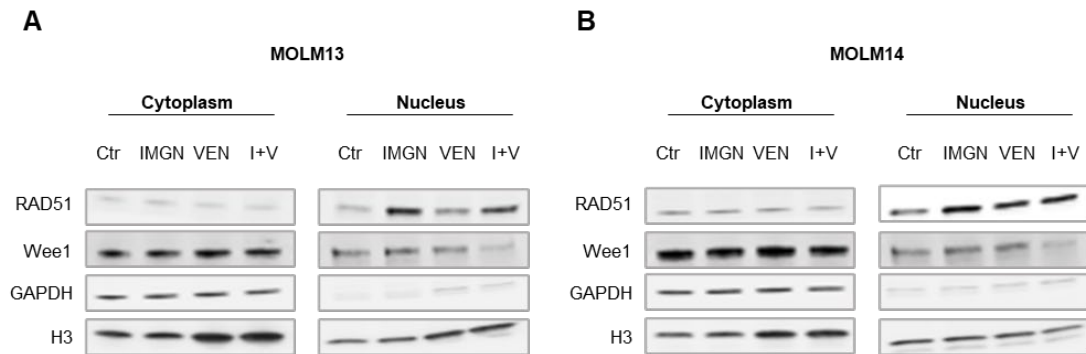


Figure 11. Western blot analysis of DNA damage response associated proteins in A) MOLM13 and B) MOLM14 AML cells treated with 2.5 ng/mL IMGN632 for 24 h and co-treated with 5 nM VEN for next 24h. Cytoplasmic and nuclear fraction was isolated using NE-PER kit (ThermoScientific).

Since pre-treatment of AML cells with IMGN632 prior to VEN administration had significant synergistic effect and exceeded the efficacy of VEN followed by IMGN632 treatment scheme, next we examined the mechanism underlying the observed discrepancy. MV4-11 AML cells were pretreated for 24h with either IMGN632 or VEN alone, followed by 24-hour exposure to IMGN632 or VEN, respectively, and subjected to immunoblotting. As shown in Figure 12, pre-treatment of AML cells with IMGN632 prior to VEN administration led to significant elevation of cleaved PARP and caspase-3, well known characteristics of apoptosis. In contrast, pre-treatment with VEN for 24h followed by IMGN632 had visibly less profound effect on induction of PARP and caspase-3. IMGN632 pretreatment induced profound phosphorylation of histone H2AX, a marker of double-stranded DNA damage, which was accompanied by increase in total and phosphorylated levels of

DNA-damage response sensor, p53. VEN pretreatment produced significantly lower levels of p- γ H2AX and did not trigger of p53 phosphorylation. These results suggest that initial activation of DDR pathway by IMGN632 may be crucial for the overall effect of dual drug combination.

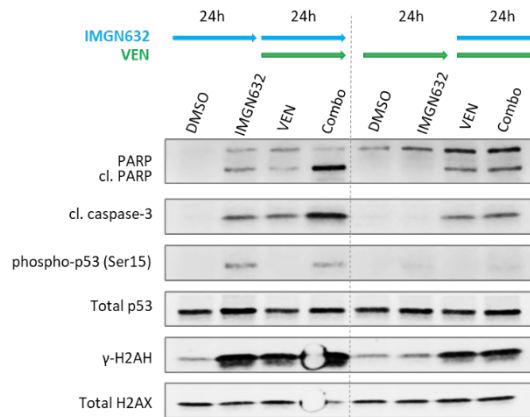


Figure 12. The effect of sequence of IMGN632 and VEN treatment in AML cells. MV4-11 AML cells were pretreated with IMGN632 for 24 h followed by 24h VEN (*left*) or pretreated with VEN for 24h followed by 24h IMGN632 (*right*). Cells were immunoblotted for the indicated proteins.

Our previous results showed that IMGN632 induced profound double-stranded DNA damage, G1 (MOLM13 and MOLM14 cells) or G2/M (MV4-11 cells) phase cell cycle arrest and decline in S-phase population, all above augmented by VEN/AZA co-treatment. However, increase in levels of double-strand DNA breaks (p-H2AX) was accompanied by apoptotic caspase-3 and PARP cleavage. Given that cytotoxic payload of IMGN632 is a DNA mono-alkylator, which does not cause direct DNA breaks, next we tested the possibility that accumulation of p-H2AX may reflect apoptotic DNA cleavage. As shown in Figure 13, co-treatment with pan-caspase inhibitor QVD-OPh, completely prevented phosphorylation of H2AX but did not change the total level of H2AX.

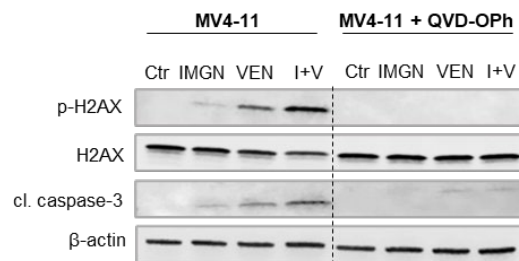


Figure 13. Western blot analysis of double-strand DNA breaks marker p-H2AX. MV411 cells were treated with 10 μ M QVD-OPh caspase inhibitor, 2.5 ng/mL IMGN632 for 24 h and co-treated with 5 nM VEN for next 24h.

In addition, caspase inhibition abolished the cytotoxic effect of IMGN632 alone or in combination with VEN (Figure 14). These results indicate that double-stranded DNA damage and p-H2AX triggered by combined treatment may be secondary events associated with apoptosis but not initial cause of cell cycle arrest.

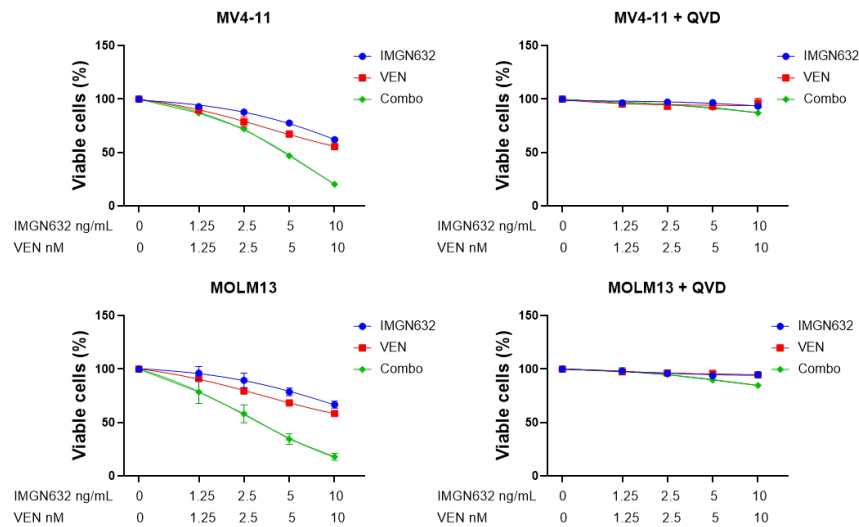


Figure 14. Caspase inhibition prevents cytotoxic effect of IMG632 and VEN combination. AML cells were treated with 10 μ M QVD-OPh caspase inhibitor, 2.5 ng/mL IMG632 for 24 h and co-treated with 5 nM VEN for next 24h. Cell viability was measured by CellTiter Glo assay.

In parallel to mechanistic studies, we also tested the activity of IMG632/VEN/AZA combination in AML cells resistant to VEN. Konopleva's lab has generated VEN resistant MOLM13 and MV4-11 (FLT3-ITD) and OCI-AML2 (wild-type FLT3) cell lines by prolonged exposure of cells to increasing doses of VEN up to 1 μ M. First, MOLM13 parental and VEN resistant were screened for CD-123 expression using anti-CD-123-PE antibody and subjected to flow cytometry analysis. Surprisingly, as shown in Figure 10A, VEN resistant cells had decreased expression of CD123 receptor. Correspondingly, these cells were significantly less sensitive to IMG632 alone in comparison to the parental cells. Triple combination of IMG632/VEN/AZA, despite a 100-fold increase in IMG632 and VEN doses was ineffective in VEN resistant MOLM13 FLT3-ITD cells. Similarly, while OCI-AML2 wild-type FLT3 were sensitive to IMG632/VEN/AZA, Ven resistant counterparts did not respond to triple treatment (Figure 15 and 16).

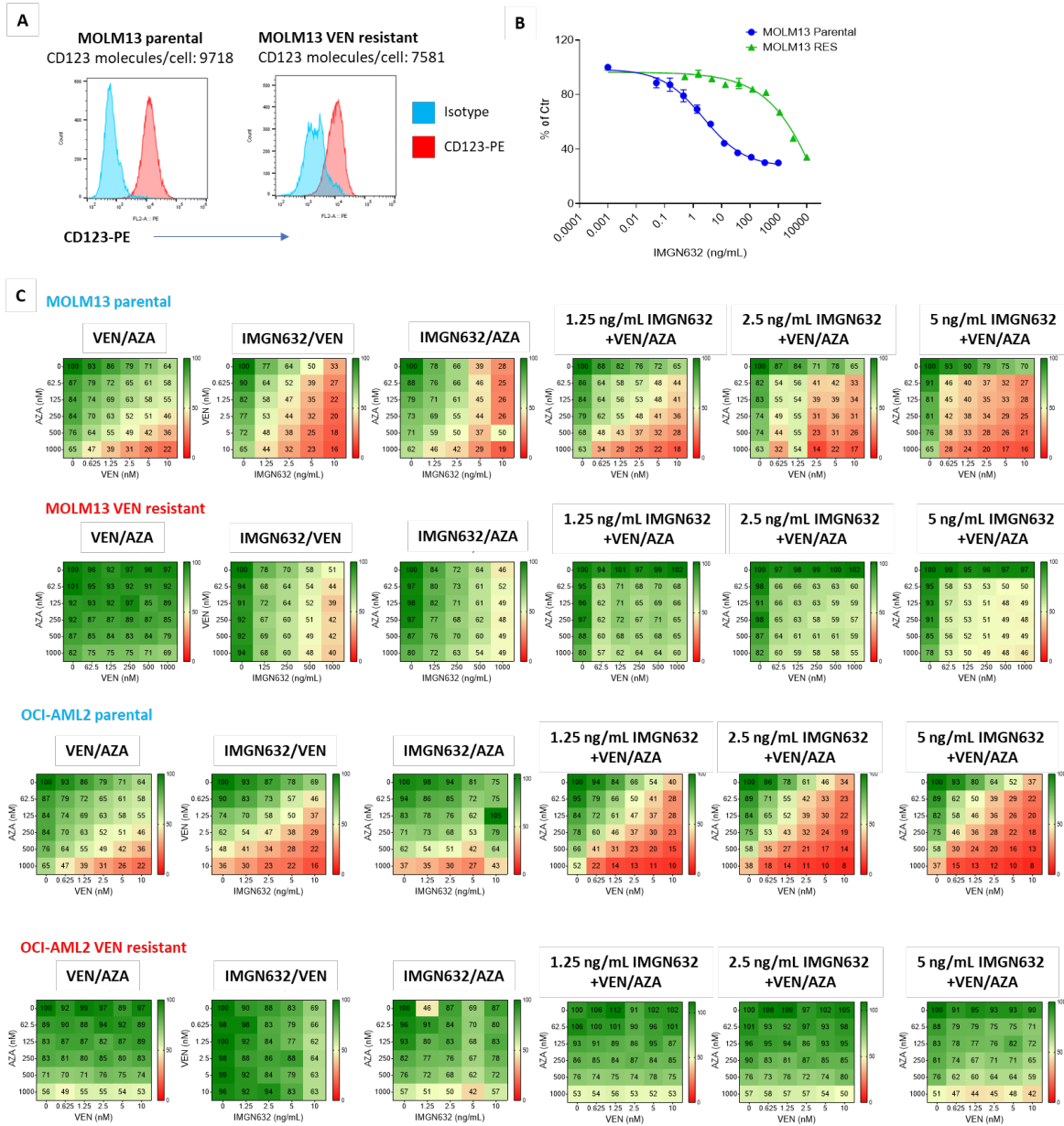


Figure 15. The efficacy of IMGN632/VEN/AZA combination in VEN resistant AML cells. (A) Flow cytometry analysis of the expression of CD123 receptor following staining with anti-CD-123-PE antibody. (B) Activity of IMGN632 in MOLM13 parental and VEN resistant cells after 24h exposure. Cell Viability was measured using CellTiterGlo assay. (C) Activity of triple IMGN632/VEN/AZA treatment in parental and VEN resistant AML cell lines. Cells were pre-treated with IMGN632 for 24h followed by 24h VEN/AZA exposure.

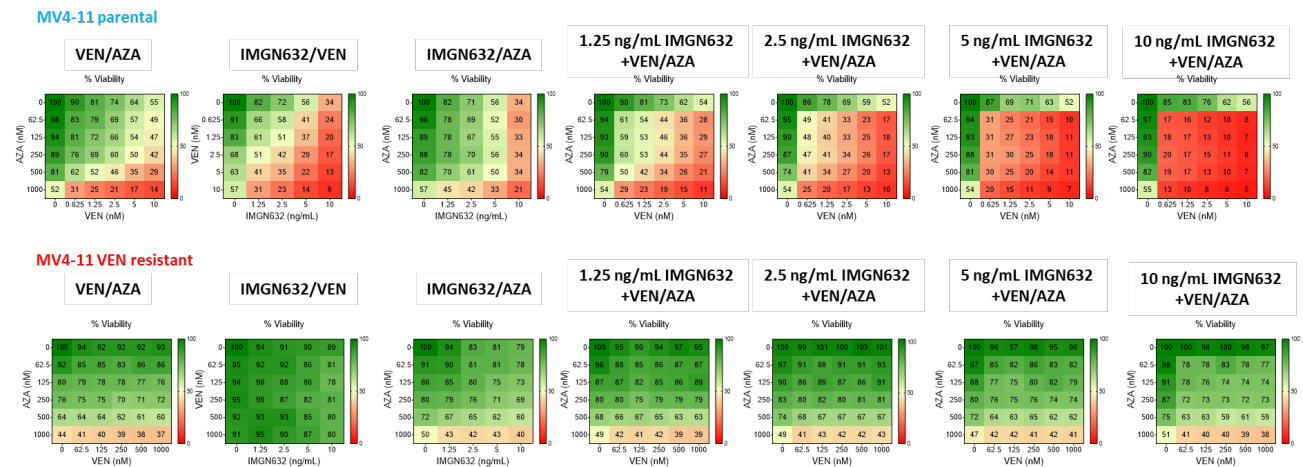


Figure 16. The efficacy of IMGN632/VEN/AZA combination in MV4-11 cells sensitive and resistant to Venetoclax. Cells were pre-treated with IMGN632 for 24h followed by 24h VEN/AZA exposure. Cell viability was measured by CTG assay.

We also tested the efficacy of triple combination in MOLM13 AML cells resistant to both VEN and AZA. Similarly, to the VEN-resistant cells, IMGN632 was not able to re-sensitize resistant cells to VEN/AZA (Figure 17).

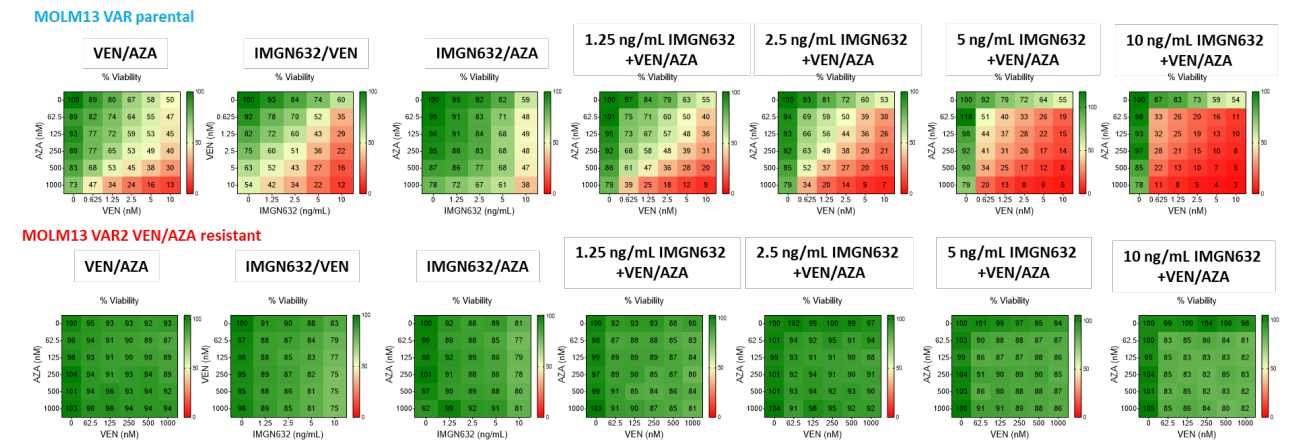


Figure 17. The efficacy of IMGN632/VEN/AZA combination in MOLM13 cells sensitive to Venetoclax and 5-Azacytidine. Cells were pre-treated with IMGN632 for 24h followed by 24h VEN/AZA exposure. Cell viability was measured by CTG assay.

Further analysis revealed that unlike parental cells, both VEN-resistant and VEN/AZA-resistant cells were significantly less sensitive to IMGN632 (Figure 17A) than their parental counterparts. Interestingly, resistant cells had significantly elevated basal level of PARP as well as phospho- and total p53 (Figure 17B). PARP is a critical enzyme involved in DNA repair and many other cellular processes including transcription and modulation of chromatin structure. PARP plays a central role in NER and BER and enables repair of DNA damage caused by DNA alkylating agents and chemotherapeutic drugs. Studies have demonstrated that PARP is upregulated in certain cancers and

its overexpression confers poor prognosis. On the other hand, p53 serves as a major transcriptional effector in the DNA damage response (DDR) signaling cascade and phosphorylation at Serine 15 is the primary step of DDR, preventing p53 from proteasomal degradation. Importantly, increased capacity for DNA repair is frequently found in cells that acquire resistance to DNA-targeting therapies. Since above components of DDR were also intrinsically upregulated in VEN and VEN/AZA resistant cells, it is plausible to hypothesize that these cells have an increased ability to repair IMGN632-induced DNA, which in turn translates into observed decrease in drug's efficacy. Upregulation of DNA repair mechanisms in VEN and VEN/AZA resistant cells may be therefore one of the potential mechanisms by which AML cells can also become resistant to IMGN632.

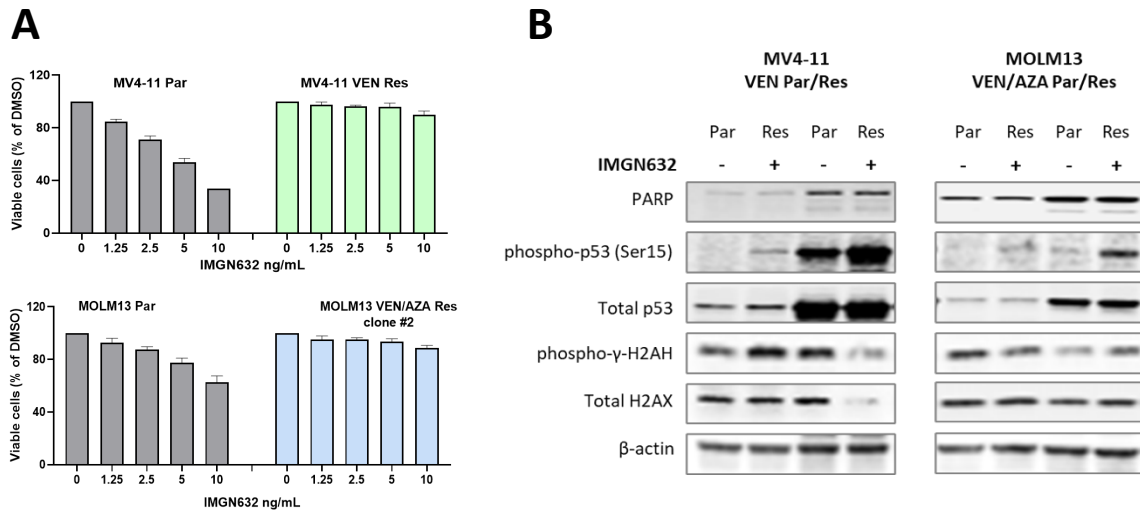


Figure 17. The efficacy of single agent IMGN632 treatment in VEN-resistant MV4-11 and VEN/AZA-resistant MOLM13 cells. A) Cell were treated with IMGN632 for 48h and cell viability was measured by CTG assay. B) Western blot analysis of DNA-damage response components in cells treated with 2.5 ng/mL of IMGN632 for 24h.

Specific Aim 2, Major Task 2: Determine the efficacy of combining anti-CD123 therapy with AZA/venetoclax *in vivo*.

Studies from this task were completed in 2021 and presented in the Annual Report 2021.

Specific Aim 2, Major Task 3:

The goal of this task is to obtain approval, activate, and enroll additional patients with BPDCN on a clinical trial testing the triplet combination of tagraxofusp, azacitidine, and venetoclax. We have made good progress on this task during the funding period. The clinical trial testing TAG/AZA or TAG/AZA/VEN for patients with acute myeloid leukemia (AML) or myelodysplastic syndrome (MDS) completed dose escalation and the recommended phase 2 dose (RP2D) was determined for the TAG/AZA/VEN triplet. This allowed us to open the expansion cohorts for patients with BPDCN

using the RPD2 of TAG/AZA/VEN, which is AZAcitidine 75 mg/m² on days 1-7, VENetoclax 400 mg daily on days 1-21, and TAG 12 ug/kg/day on days 4-6.

We opened two arms for patients with BPDCN, one for first line treatment and one for relapsed or refractory BPDCN. To date, 7 patients with r/r BPDCN have been enrolled and 7 patients with previously untreated BPDCN has been enrolled. This is 8 new BPDCN enrollments in the last year. Correlative samples are being collected from all patients for future laboratory analysis. The analysis is ongoing, but we are seeing encouraging results. These include that there is no obvious difference in adverse events between patients with BPDCN and the prior dose-finding cohorts of patients with AML. Enrollment is continuing (goal 16 per cohort) and survival analysis will follow. Overall, we are very pleased with our progress and we continue to enroll subjects with BPDCN.

Aim 3

More than 50% of patients with BPDCN carry a mutation affecting an RNA splicing factor. Splicing factor mutations in BPDCN and related myeloid neoplasms are concentrated in four genes (*SF3B1*, *SRSF2*, *U2AF1*, and *ZRSR2*), are mutually exclusive with one another, and result in wide-spread changes in isoform expression. Mutations in splicing factors seen in BPDCN alter RNA splicing in a manner that skews usage of annotated RNA isoforms or promote expression of novel, unannotated RNA isoforms which either are degraded by NMD or stable protein-coding transcripts (“NMD neutral” events; **Fig.18A**). These mutations generate hundreds to thousands of RNA mis-splicing events in tandem. Consequently, comprehensive evaluation of these alterations in a high-throughput manner has not been done due to the challenges of performing such studies. Dissecting the functionally important mis-splicing events generated by mutant RNA splicing factors is important as this effort will illuminate myeloid pathogenesis and inform development of new therapies targeting the aberrant proteins and pathways induced by these mutations. Previous work from our lab has performed positive enrichment CRISPR screens targeting the genes whose mRNA undergo NMD to evaluate NMD-inducing mis-splicing events in a high-throughput manner. However, NMD-neutral mis-splicing events have not been evaluated a similar large-scale manner. We therefore hypothesized that BPDCN-associated mutations in RNA splicing factors drive disease development through generation of novel, stably expressed proteins and that understanding the biology of isoforms will result in the development of novel therapeutics for MDS patients.

To this hypothesis we generated a DNA barcoded open-reading frame (ORF) library encoding 252 transcripts whose mRNA splicing are altered by MDS-associated mutations in *SF3B1*, *U2AF1*, or *SRSF2*. This library consisted of cDNAs encoding the largest annotated RNA isoform of each gene (121 cDNAs), the MDS-associated altered isoform (121 cDNAs; **Fig.18B-C**), positive control cDNAs which promote myeloid leukemia cell proliferation (NRas^{G12D} and cKit^{D816V}), negative control cDNAs which impair cell proliferation (BAX and TP53), and neutral control cDNAs (mCherry and luciferase). Each was cloned into MSCV-IRES-GFP plasmid with a flanking barcode allowing for cDNA identification and quantification via next-generation sequencing. As a proof-of-concept, our cDNA library was initially expressed in cytokine-dependent hematopoietic cell lines *in vitro* as well as human AML cell lines which can be induced for myeloid differentiation (**Fig.18B**). Our approach successfully identified expected positive/negative control cDNAs as well as potential aberrant RNA

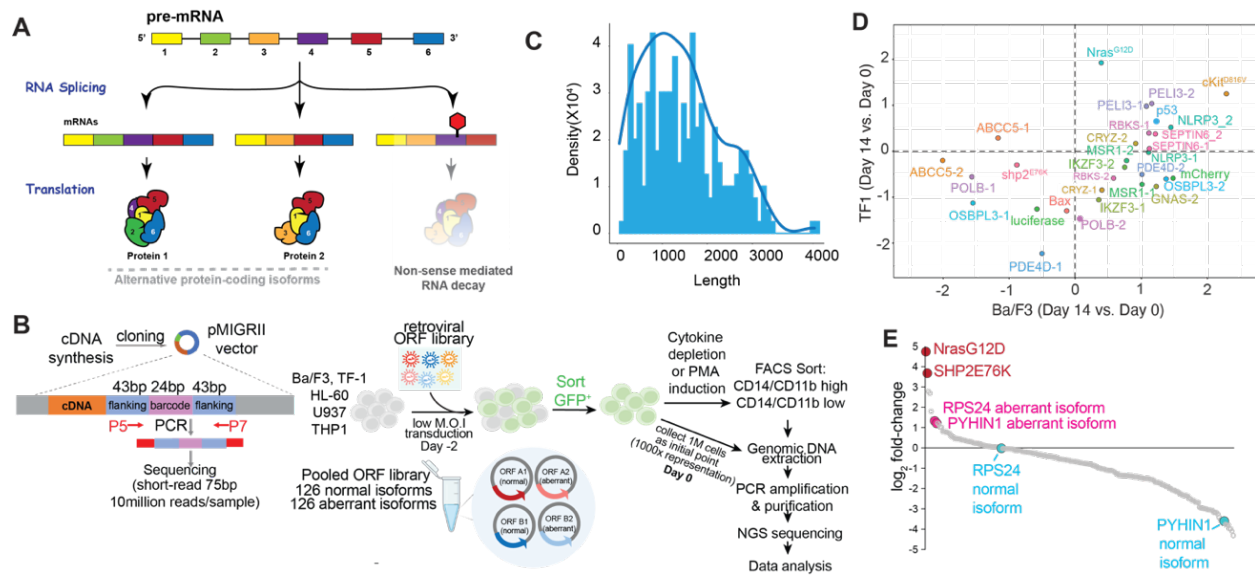


Fig. 18. Splice variant cDNA screen to identify aberrant isoforms regulating cell growth and myeloid differentiation in splicing factor mutant MDS. (A) Schema of the impact of aberrant RNA splicing on RNA transcripts. Aberrant splicing could result in production of stable, protein-producing RNA isoforms (either annotated or unannotated isoforms) or production of an mRNA which is degraded by non-sense mediated RNA decay (NMD). This proposal is aimed at systematically evaluating potentially oncogenic protein-producing RNA isoforms. **(B)** Design of DNA-barcoded open-reading frame (ORF) library encoding 252 transcripts of RNA mis-splicing and experimental flow of *in vitro* cytokine-independent growth and differentiation screens. **(C)** ORF length distribution. **(D)** Correlation of enrichment scores of isoforms between TF1 and Ba/F3 cells in cytokine depletion screen. **(E)** Log₂ (fold-change) of cDNAs screen in TF1 cells at day 28 of cytokine depletion versus day 0. Positive and negative controls highlighted in orange and blue respectively.

isoforms associated with enhanced cytokine-independent growth and/or impaired terminal myeloid differentiation (**Fig.18D-E**).

In vitro studies were followed by *in vivo* screens in bone marrow cells from C57/B6 wild-type (WT) as well as *Tet2* knockout (KO) mice. We evaluated those cDNAs enriched in distinct cell populations (including peripheral blood CD11b⁺ and B220⁺ cells) as well as bone marrow CD11b⁺, B220⁺, and Lin-cKit⁺ hematopoietic progenitors following long-term engraftment *in vivo* (**Fig.19A-C**). This identified a number of candidate aberrant RNA splicing isoforms which promote myeloid and HSPC expansion compared with the normal/annotated isoform counterparts. Interestingly, a number of these enriched aberrant isoforms function in IFN-dependent immune signaling (IFI144, IFI44L, and SPPL2A), the inflammasome (NLRP3), and RNA modifications (METTL15). Of note, IFI44, IFI44L, and SPPL2A mis-splicing events are all driven by U2AF1^{S34} and U2AF1^{Q157} mutants. U2AF1 mutations confer poor prognosis with MDS patients. Therefore, we are now focused on understanding of the functions of SPPL2A, IFI44, and IFI44L aberrant isoforms.

SPPL2a is localized in membranes of lysosomes and late endosomes and cleaves N-terminal fragments of CD74. Mis-splicing of SPPL2A driven by U2AF1 S34 and Q157 mutations leads to exon 11 skipping and removal of SPPL2A's fourth cytosolic domain, the site responsible for the catalytic function of SPPL2A. We therefore hypothesize that CD74 cleavage and MHC class II presentation is dampened by SPPL2A aberrant isoform usage. We will next determine the enzymatic activity of SPPL2A isoforms using an established β GEFC reporter system for CD74 cleavage. To assess roles of SPPL2A isoforms on MHC class II activities, SPPL2A isoforms will be ectopically expressed in SPPL2A-null MOLM13, MV4-11, and OCI-AML3 cells and MHC class II (HLA-DR,

DQ, and DP) surface levels will be measured in presence or absence of IFN γ (a cytokine which upregulates MHC II) by flow cytometry. Finally, to test the ability of SPPL2A aberrant isoform to regulate antigen presentation and CD4 T cell activation, DO-11-10 CD4 T cell-based antigen presentation assay will be employed. Murine AML cell lines C1498 and RN2 ectopically expressing SPPL2A isoforms will be incubated with the ovalbumin peptide (OVA-323-339) to facilitate OVA antigen presentation on I-A^b MHC II. These cells will be co-cultured with DO-11.10 murine CD4 cells and CD4 cell activation will be evaluated by IL-2 secretion and CD25 expression.

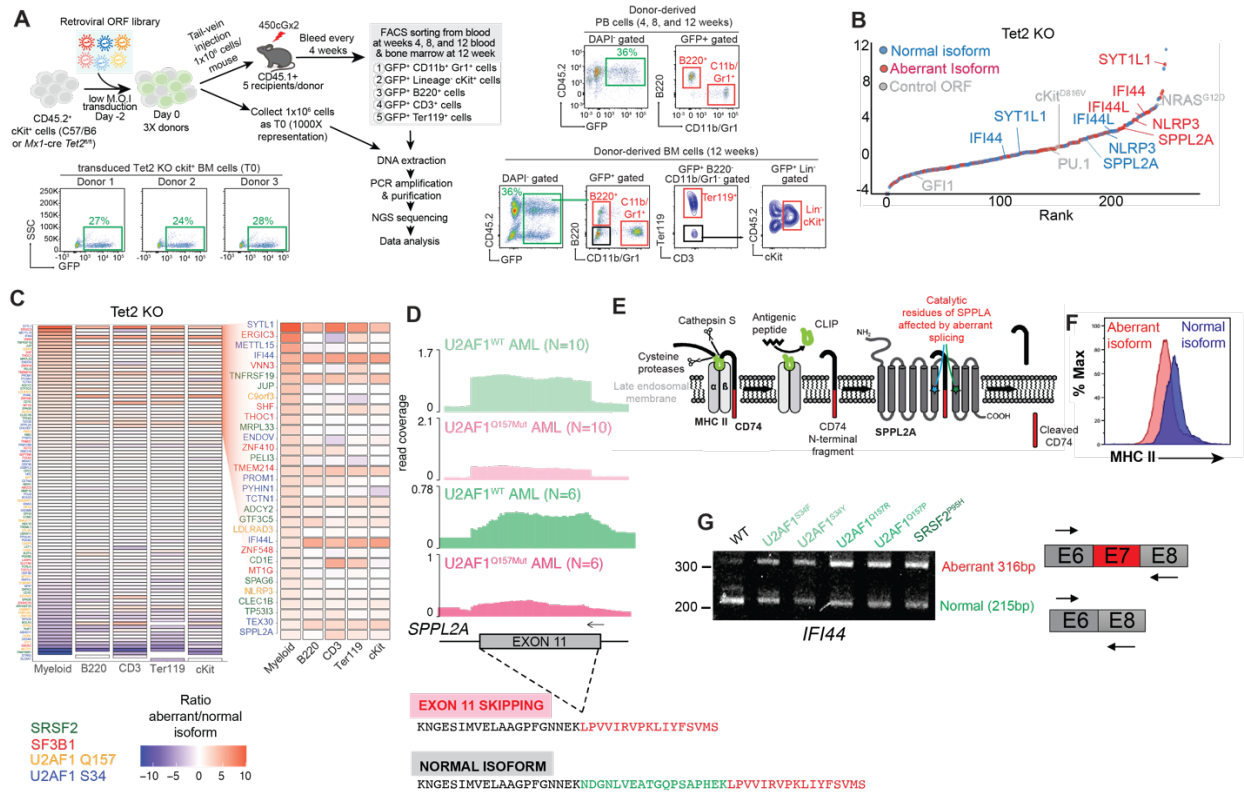


Fig. 2. Identification of aberrant isoforms driving *in vivo* clonal expansion. (A) Schema of *in vivo* cDNA screen in Tet2 KO and WT progenitor-engrafted mouse models. Sorting strategies for different cell types are highlighted. (B) \log_2 (fold-change) values of cDNAs in myeloid cells from Tet2 KO mouse *in vivo* screen. (C) Heatmap for ratio of aberrant/normal isoform enrichment in each cell type from peripheral blood (PB) or bone marrow (BM) at week 12 versus time 0. Mis-spliced genes are colored based on their induction by each MDS-associated RNA splicing factor mutation. (D) RNA-seq coverage plots in two distinct AML patient cohorts wild-type or mutant for U2AF1^{Q157} mutations at SPPL2A demonstrating exon 11 skipping in the U2AF1 mutants. (E) Schema of the role of SPPL2A on CD74 cleavage which allows for MHC class II antigen loading, release from endosome, and cell surface localization. (F) MHC class II surface abundance in mouse c-Kit⁺ cells expressing normal or aberrant SPPL2A isoforms. (G) RT-PCR of IFI144 exons 6-8 in isogenic K562 cells with distinct knockin U2AF1 or SRSF2 mutations demonstrating exon 7 inclusion driven by the mutants.

What opportunities for training and professional development has the project provided?

Nothing to report

How were the results disseminated to communities of interest?

We have presented following posters at the national meetings:

2020 ASH

Combining IMGN632, a Novel CD123-Targeting Antibody Drug Conjugate with Azacitidine and Venetoclax Facilitates Apoptosis *in Vitro* and Prolongs Survival *In Vivo* in AML Models

<https://www.sciencedirect.com/science/article/pii/S0006497118720326>

2020 SOHO

AML-367: IMGN632, a CD123-Targeting ADC Bearing a DNA-Alkylating IGN Payload, Combines Effectively as a Triplet Regimen with Azacitidine and Venetoclax In Vivo, Prolonging Survival in Preclinical Models of Human Acute Myeloid Leukemia (AML)

<https://www.sciencedirect.com/science/article/pii/S2152265020307680>

2019 ASH

IMGN632, a CD123-Alkylating ADC Bearing a DNA Alkylating IGN Payload, Combines Effectively with Azacitidine and Venetoclax In Vivo, Prolonging Survival in Preclinical Models of Human Acute Myeloid Leukemia (AML)

https://ashpublications.org/blood/article/134/Supplement_1/1375/427254/IMGN632-a-CD123-Alkylating-ADC-Bearing-a-DNA

2019 EHA

PF201 THE COMBINATION OF IMGN632, A CD123-TARGETING ADC, WITH VENETOCLAX ENHANCES ANTI-LEUKEMIC ACTIVITY IN VITRO AND PROLONGS SURVIVAL IN VIVO IN PRE-CLINICAL MODELS OF HUMAN AML

https://journals.lww.com/hemasphere/Abstract/2019/06001/PF201_THE_COMBINATION_OF_IMGN632,_A.101.aspx

2018 ASH

Pre-Clinical Efficacy of CD123-Targeting Antibody-Drug Conjugate IMG632 in Blastic Plasmacytoid Dendritic Cell Neoplasm (BPDCN) Models

<https://www.sciencedirect.com/science/article/pii/S0006497119400566>

Conference abstract oral presentation:

Togami K, Chung SS, Madan V, Kenyon CM, Cabal-Hierro L, Taylor J, Kim SS, Griffin GK, Ghandi M, Li J, Li YY, Angelot-Delettre F, Biichle S, Seiler M, Buonamici S, Lovitch SB, Louissaint A, Moran EA, Jardin F, Piccaluga PP, Weinstock DM, Hammerman PS, Yang H, Konopleva M, Pemmaraju N, Garnache-Ottou F, Abdel-Wahab O, Koeffler P, Lane AA. Male-Biased Spliceosome Mutations in Blastic Plasmacytoid Dendritic Cell Neoplasm (BPDCN) Impair pDC Activation and Apoptosis. Oral presentation. American Society of Hematology Annual Meeting 2020. *Blood* (2020) 136 (Supplement 1): 13–14. <https://doi.org/10.1182/blood-2020-137727>

Published paper:

Togami K, Chung SS, Madan V, Booth CAG, Kenyon CM, Cabal-Hierro L, Taylor J, Kim SS, Griffin GK, Ghandi M, Li J, Li YY, Angelot-Delettre F, Biichle S, Seiler M, Buonamici S, Lovitch SB, Louissaint A, Moran EA, Jardin F, Piccaluga PP, Weinstock DM, Hammerman PS, Yang H, Konopleva M, Pemmaraju N, Garnache-Ottou F, Abdel-Wahab O, Koeffler P, Lane AA. Sex-biased *ZRSR2* mutations in myeloid malignancies impair plasmacytoid dendritic cell activation and apoptosis. *Cancer Discovery*. 2022 Feb;12(2):522-541. doi: 10.1158/2159-8290.CD-20-1513. PMID: 34615655

Published paper:

Griffin GK, Booth CAG, Togami K, Chung SS, Ssozi D, Verga JA, Bouyssou JM, Lee YS, Shanmugam V, Hornick JL, LeBoeuf NR, Morgan EA, Bernstein BE, Hovestadt V, van Galen P, Lane AA. Ultraviolet radiation shapes dendritic cell leukaemia transformation in the skin. *Nature*. 2023 Jun;618(7966):834-841. doi: 10.1038/s41586-023-06156-8. Epub 2023 Jun 7. PMID: 37286599; PMCID: PMC10284703.

Conference abstract oral presentation:

2020 ASH

ZRSR2 Mutation Induced Minor Intron Retention Drives MDS and Diverse Cancer Predisposition Via Aberrant Splicing of *LZTR1*

<https://ash.confex.com/ash/2020/webprogram/Paper136445.html>

2021 ASH

Modulation of RNA Splicing Enhances Response to BCL2 Inhibition in Acute Myeloid Leukemia

<https://ashpublications.org/blood/article/138/Supplement%201/507/479370/Modulation-of-RNA-Splicing-Enhances-Response-to?searchresult=1>

(Dr. Abdel-Wahab)

Published paper:

Chen S, Vedula RS, Cuevas-Navarro A, Lu B, Hogg SJ, Wang E, Benbarche S, Knorr K, Kim WJ, Stanley RF, Cho H, Erickson C, Singer M, Cui D, Tittley S, Durham BH, Pavletich TS, Fiala E, Walsh MF, Inoue D, Monette S, Taylor J, Rosen N, McCormick F, Lindsley RC, Castel P, **Abdel-Wahab O**. Impaired proteolysis

of non-canonical RAS proteins drives clonal hematopoietic transformation. *Cancer Discov.* 2022 Jul 29;CD-21-1631. doi: 10.1158/2159-8290.CD-21-1631. Epub ahead of print. PMID: 35904492.

Wang E, Pineda JMB, Kim WJ, Chen S, Bourcier J, Stahl M, Hogg SJ, Bewersdorf JP, Han C, Singer ME, Cui D, Erickson CE, Tittley SM, Penson AV, Knorr K, Stanley RF, Rahman J, Krishnamoorthy G, Fagin JA, Creger E, McMillan E, Mak CC, Jarvis M, Bossard C, Beaupre DM, Bradley RK, **Abdel-Wahab O**. Modulation of RNA splicing enhances response to BCL2 inhibition in leukemia. *Cancer Cell.* 2022 Dec 17:S1535-6108(22)00588-8. doi: 10.1016/j.ccell.2022.12.002. Epub ahead of print. PMID: 36563682.

Knorr K, Rahman J, Erickson C, Wang E, Monetti M, Li Z, Ortiz-Pacheco J, Jones A, Lu SX, Stanley RF, Baez M, Fox N, Castro C, Marino AE, Jiang C, Penson A, Hogg SJ, Mi X, Nakajima H, Kunitomo H, Nishimura K, Inoue D, Greenbaum B, Knorr D, Ravetch J*, **Abdel-Wahab O***. Systematic evaluation of AML-associated antigens identifies anti-U5 SNRNP200 therapeutic antibodies for the treatment of acute myeloid leukemia. *Nat Cancer.* 2023 Oct 23. doi: 10.1038/s43018-023-00656-2. Epub ahead of print. PMID: 37872381. ***Co-corresponding**

What do you plan to do during the next reporting period to accomplish the goals?

Aim 1:

- Continue to study the role of KHSRP in therapy sensitivity and resistance and whether it is necessary and/or sufficient by performing additional add-back rescue control experiments, including with domain mutants of KHSRP.
- Continue to study the relationship between KHSRP and SLC23A1, including asking if KHSRP modulates the level of SLC23A1, and whether this is via transcription, translation, or post-translational mechanisms.
- Determine if Vitamin C affects BPDCN drug sensitivity and whether this is via a KHSRP/SLC23A1 axis. Explore alternative hypotheses considering that SLC23A1 may transport other solutes that could be important in the therapeutic effect.
- Test if KHSRP and/or Vitamin C are relevant to any drug sensitivity in BPDCN cells, or whether this is specific to the two treatments we have tested already, VEN/AZA and tagraxofusp.
- Test if this same molecular mechanism is relevant in other acute leukemias (e.g., AML/ALL) in the setting of MRD/residual disease, or if it is restricted to BPDCN. If restricted, begin to explore features that influence this dependency.
- Continue to mine the other hits from BPDCN CRISPRi in the setting of treatment and the MRD state to define additional targets for sensitization or resistance experimental follow up.

Aim 2, Sub-Aim 1:

- We will continue to analyze the effect of IMGN632/VEN combination on key signaling pathways involved in DDR: homologous recombination and non-homologous end joining with particular emphasis on the role of sequence of IMGN and VEN administration.

- We will perform RNAseq to determine the effect of VEN on the suppression of DNA-damage response (DDR) induced by IMGN632.
- We will determine the role of IMGN632-mediated suppression of ATM/Chk2 pathway and activation of Rad51 to overall effect of IMGN632/VEN combination

Aim 2, Sub-Aim 3:

- We will continue to enroll patients with BPDCN to the frontline and relapsed/refractory cohorts. We will continue to collect and process samples for laboratory correlative analyses.

Aim 3

- Test the functional relevance of SPPL2A splicing on MHC II surface abundance and antigen presentation in BPDCN.
- Test the importance of IFI44 and IFI44L splicing on BPDCN cell growth and signaling.
- Complete preclinical studies of DYRK/CLK inhibition in BPDCN PDX models.

4. IMPACT:

What was the impact on the development of the principal discipline(s) of the project?

Nothing to Report

What was the impact on other disciplines?

Nothing to Report

What was the impact on technology transfer?

Nothing to Report

What was the impact on society beyond science and technology?

Nothing to Report

Changes in approach and reasons for change

Nothing to Report

Actual or anticipated problems or delays and actions or plans to resolve them

Nothing to Report

Changes that had a significant impact on expenditures

Nothing to Report

Significant changes in use or care of human subjects, vertebrate animals, biohazards, and/or select agents

Nothing to Report

Significant changes in use or care of human subjects

Nothing to Report

Significant changes in use or care of vertebrate animals

Nothing to Report

Significant changes in use of biohazards and/or select agents

Nothing to Report

5. PRODUCTS:

- **Publications, conference papers, and presentations**

- Journal publications.**

Conference abstract oral presentation (Lane):

Togami K, Chung SS, Madan V, Kenyon CM, Cabal-Hierro L, Taylor J, Kim SS, Griffin GK, Ghandi M, Li J, Li YY, Angelot-Delettre F, Biichle S, Seiler M, Buonamici S, Lovitch SB, Louissaint A, Moran EA, Jardin F, Piccaluga PP, Weinstock DM, Hammerman PS, Yang H, Konopleva M, Pemmaraju N, Garnache-Ottou F, Abdel-Wahab O, Koeffler P, Lane AA. Male-Biased Spliceosome Mutations in Blastic Plasmacytoid Dendritic Cell Neoplasm (BPDCN) Impair pDC Activation and Apoptosis. Oral presentation. American Society of Hematology Annual Meeting 2020. *Blood* (2020) 136 (Supplement 1): 13–14. <https://doi.org/10.1182/blood-2020-137727>

Published papers:

Togami K, Chung SS, Madan V, Booth CAG, Kenyon CM, Cabal-Hierro L, Taylor J, Kim SS, Griffin GK, Ghandi M, Li J, Li YY, Angelot-Delettre F, Biichle S, Seiler M, Buonamici S, Lovitch SB, Louissaint A, Moran EA, Jardin F, Piccaluga PP, Weinstock DM, Hammerman PS, Yang H, Konopleva M, Pemmaraju N, Garnache-Ottou F, Abdel-Wahab O, Koeffler P, Lane AA. Sex-biased *ZRSR2* mutations in myeloid malignancies impair plasmacytoid dendritic cell activation and apoptosis. *Cancer Discovery*. 2021; doi: 0.1158/2159-8290. CD-20-1513. Online ahead of print. PMID: 34615655

Griffin GK, Booth CAG, Togami K, Chung SS, Ssozi D, Verga JA, Bouyssou JM, Lee YS, Shanmugam V, Hornick JL, LeBoeuf NR, Morgan EA, Bernstein BE, Hovestadt V, van Galen P, Lane AA. Ultraviolet radiation shapes dendritic cell leukaemia transformation in the skin. *Nature*. 2023 Jun;618(7966):834-841. doi: 10.1038/s41586-023-06156-8. Epub 2023 Jun 7. PMID: 37286599; PMCID: PMC10284703.

Chen S, Vedula RS, Cuevas-Navarro A, Lu B, Hogg SJ, Wang E, Benbarche S, Knorr K, Kim WJ, Stanley RF, Cho H, Erickson C, Singer M, Cui D, Tittley S, Durham BH, Pavletich TS, Fiala E, Walsh MF, Inoue D, Monette S, Taylor J, Rosen N, McCormick F, Lindsley RC, Castel P, **Abdel-Wahab O**. Impaired proteolysis of non-canonical RAS proteins drives clonal hematopoietic transformation. *Cancer Discov*. 2022 Jul 29;CD-21-1631. doi: 10.1158/2159-8290.CD-21-1631. Epub ahead of print. PMID: 35904492.

Wang E, Pineda JMB, Kim WJ, Chen S, Bourcier J, Stahl M, Hogg SJ, Bewersdorf JP, Han C, Singer ME, Cui D, Erickson CE, Tittley SM, Penson AV, Knorr K, Stanley RF, Rahman J, Krishnamoorthy G, Fagin JA, Creger E, McMillan E, Mak CC, Jarvis M, Bossard C, Beaupre DM, Bradley RK, **Abdel-Wahab O**. Modulation of RNA splicing enhances response to BCL2 inhibition in leukemia. *Cancer Cell*. 2022 Dec 17:S1535-6108(22)00588-8. doi: 10.1016/j.ccell.2022.12.002. Epub ahead of print. PMID: 36563682.

Acknowledgement of federal support: Yes

Books or other non-periodical, one-time publications.

Nothing to Report

Other publications, conference papers and presentations.

Nothing to Report

- **Website(s) or other Internet site(s)**

Nothing to Report

- **Technologies or techniques**

Nothing to Report

- **Inventions, patent applications, and/or licenses**

Nothing to Report

- **Other Products**

Nothing to Report

6. PARTICIPANTS & OTHER COLLABORATING ORGANIZATIONS

What individuals have worked on the project?

DFCI

Name: Andrew Lane, MD, PhD
Project Role: Site PI (DFCI)
Researcher Identifier (e.g. ORCID ID):
Nearest person month worked: 0.77 person-months per year
Contribution to Project: Dr. Lane supervised the project and worked on development and regulatory items for the clinical protocol.

Name: Hayden Bell, PhD
Project Role: Postdoctoral fellow
Researcher Identifier (e.g. ORCID ID):
Nearest person month worked: 1 person-months per year
Contribution to Project: Dr. Bell performed experiments in the laboratory and worked to develop platforms for integrated analysis of leukemia informatics data.

Name: Siobhan Rice, PhD
Project Role: Postdoctoral fellow
Researcher Identifier (e.g. ORCID ID):
Nearest person month worked: 10 person-months per year
Contribution to Project: Dr. Rice worked to optimize CRISPR editing in blood cells and assisted with informatic analysis of next generation sequencing data.

Name: Jenalyn Weekes
Project Role: Research Technician
Researcher Identifier (e.g. ORCID ID):
Nearest person month worked: 4.5 person-months per year
Contribution to Project: Ms. Weekes worked on processing correlative samples from patients and assisting on laboratory studies of therapy resistance.

MDACC

Name: Marina Konopleva, MD, PhD
Project Role: Site PI (MDACC)
Researcher Identifier (e.g. ORCID ID):
Nearest person month worked: 1 (rounded for this quarter; 0.6 person-months per year)
Contribution to Project: Dr. Konopleva designed and supervised the project

Name: Naveen Pemmaraju, MD
Project Role: Site Co-I (MDACC)
Researcher Identifier (e.g. ORCID ID):
Nearest person month worked: 1 (rounded for this quarter; 0.6 person-months per year)
Contribution to Project: Dr. Pemmaraju worked on development of the clinical protocol.

Name: Lina Han, MD, PhD
Project Role: Site Co-I (MDACC)
Researcher Identifier (e.g. ORCID ID):
Nearest person month worked: 2.4 (rounded for this quarter; 2.4 person-months per year)
Contribution to Project: Dr. Han performed benchwork and analysis of CyTOF data.

Name: Xuelin Huang, PhD
Project Role: Site Co-I (MDACC)
Researcher Identifier (e.g. ORCID ID):
Nearest person month worked: 1 (rounded for this quarter; 0.36 person-months per year)
Contribution to Project: Dr. Huang has supervised biostatistical analysis and assisted with protocol statistical design

Name: Graciela Nogueras Gonzalez
Project Role: Sr. Stat Analyst (MDACC)
Researcher Identifier (e.g. ORCID ID):
Nearest person month worked: 1 (rounded for this quarter; 0.6 person-months per year)
Contribution to Project: Performed biostatistical analysis

Name: Qi Zhang, PhD
Project Role: Postdoctoral fellow
Researcher Identifier (e.g. ORCID ID):
Nearest person month worked: 3 (rounded for this quarter; 3 person-months per year)
Contribution to Project: Dr. Zhang performed in vitro and in vivo experiments

Name: Anna Skwarska, PhD
Project Role: Instructor
Researcher Identifier (e.g. ORCID ID):
Nearest person month worked: 6 (rounded for this quarter; 6 person-months per year)
Contribution to Project: Dr. Skwarska performed in vitro experiments

MSK

Name: Omar Abdel-Wahab, MD
Project Role: Site PI (MSK)
Researcher Identifier (e.g. ORCID ID):
Nearest person month worked: 1 (rounded for this quarter; 0.6 person-months per year)
Contribution to Project: Dr. Abdel-Wahab designed and supervised the project.

Name: Pu Zhang, PhD
Project Role: Postdoctoral fellow
Researcher Identifier (e.g. ORCID ID):
Nearest person month worked: 3 (rounded for this quarter; 3 person-months per year)
Contribution to Project: Dr. Zhang performed in vitro and in vivo experiments.

Has there been a change in the active other support of the PD/PI(s) or senior/key personnel since the last reporting period?

Dr. Chen left MSK to start her own laboratory at Shanghai General Hospital, Shanghai Jiao Tong University School of Medicine, Shanghai, China. Her work and role in this grant has been taken over by Dr. Pu Zhang, a new postdoctoral fellow in the Abdel-Wahab laboratory.

One New project has been awarded for Dr. Lane since the last report:

* Title Identifying, Understanding, and Eradicating Measurable Residual Disease (MRD) in Patients

with Acute Myeloid Leukemia (AML)

Major Goals Aim 1 - Develop novel clinical-grade assays to detect and quantify AML MRD.

Aim 2 - Test novel clinical strategies to target MRD and prospectively evaluate MRD detection tools.

Aim 3 - Identify cell and environment adaptations that facilitate MRD persistence and therapy escape.

* Status of Support Active

Project Number N/A

Name of PD/PI Andrew Lane (PI)
* Source of Support Break Through Cancer
* Primary Place of Performance Dana-Farber Cancer Institute
Project/Proposal Start Date 2/01/2023 Project/Proposal End Date 1/31/2026
* Total Award Amount (including IDC)
Overlap: None
Person Months (Calendar/Academic/Summer) per budget period.
Year (YYYY) Person Months (##.##)
1. 2024 0.24 calendar
2. 2025 0.24 calendar
3. 2026 0.24 calendar

What other organizations were involved as partners?

Nothing to Report

7. SPECIAL REPORTING REQUIREMENTS

COLLABORATIVE AWARDS:

QUAD CHARTS:

8. APPENDICES: N/A